Evolution of the East Philippine Arc: Experimental constraints on magmatic phase relations and adakitic melt formation

B. Coldwell[1], J. Adam[1], T. Rushmer[1], C.G. Macpherson[2]

[1] ARC National Key Centre for the Geochemical Evolution and Metallogeny of Continents, Department of Earth and Planetary Sciences, Macquarie University, N. S. W., 2109, Australia

[2] Department of Earth Science, University of Durham, Durham, DH1 3LE, UK

Abstract:

Piston-cylinder experiments on a Pleistocene adakite from Mindanao in the Philippines have been used to establish near- and sub-liquidus phase relationships relevant to conditions in the East Philippines subduction zone. The experimental starting material belongs to a consanguineous suite of adakitic andesites. Experiments were conducted at pressures from 0.5 to 2 GPa and temperatures from 950 to 1150 °C. With 5 wt. % of dissolved H_2O in the starting mix, garnet, clinopyroxene and orthopyroxene are liquidus phases at pressures above 1.5 GPa, whereas clinopyroxene and orthopyroxene are liquidus (or near-liquidus) phases at pressures < 1.5 GPa. Although amphibole is not a liquidus phase under any of the conditions examined, it is stable under sub-liquidus conditions at temperature ≤ 1050 ºC and pressures up to 1.5 GPa. When combined with petrographic observations and bulk rock chemical data for the Mindanao adakites, these findings are consistent with polybaric fractionation that initially involved garnet (at pressures > 1.5 GPa) and subsequently involved the lower pressure fractionation of amphibole, plagioclase and subordinate clinopyroxene. Thus the distinctive Y and HREE depletions of the andesitic adakites (which distinguish them from associated non-adakitic andesites) must be established relatively early in the fractionation process. Our experiments show that this early fractionation must have occurred at pressures > 1.5 GPa and, thus, deeper than the Mindanao Moho. Published thermal models of the Philippine Sea Plate preclude a direct origin by melting of the subducting ocean crust. Thus our results favour a model whereby basaltic arc melt underwent high-pressure crystal fractionation while stalled beneath immature arc lithosphere. This produced residual magma of adakitic character which underwent further fractionation at relatively low (i.e. crustal) pressures before being erupted.

Key words: adakite, volcanic arc, crystal fractionation, Philippines, Surigao

Introduction

Adakite is a term applied to subduction-related intermediate igneous rocks that have strong heavy rare earth element (HREE) and Y depletions (and, hence elevated La/Yb and Sr/Yb) with respect to typical subduction zone andesites and dacites. They are also characteristically enriched in Mg and Ni. The original definition (Defant and Drummond 1990) specified generation above (and hence implied melting of) young subducting oceanic lithosphere in which residual garnet (± amphibole) would retain HREE. The resulting intermediate magma would subsequently acquire excess Mg and Ni during passage through the peridotitic mantle wedge (Defant and Drummond 1990; Martin et al. 2005). In spite of this generic definition, an increasing number of adakite occurrences have been identified that do not meet the geodynamic specifications of generation above a young slab (<10 Ma). This has resulted in alternative models of adakite genesis that advocate the fractionation of garnet and/or amphibole-bearing mineral assemblages from typical arc basaltic magmas or rocks (e.g. Atherton and Petford 1993; Castillo et al. 1999; Garrison and Davidson 2003; Tulloch and Kimbrough 2003; Chiaradia et al. 2004; Macpherson et al. 2006; Macpherson 2008). Eiler et al. (2007) proposed a further possibility; this was that adakitic magma might be produced by very low degrees of partial melting of mantle wedge peridotite.

Although a minor component (by volume) of most Phanerozoic arcs, adakites have the potential to provide important constraints on both modern and ancient geodynamic regimes. This is because the particular conditions required for their generation will reflect conditions and processes in their source regions. For example, dependent on their mode of formation, adakites have the potential to provide constraints on: (a) conditions of slab-melting [as predicted by several recent conceptual simulations of subduction (e.g. Gerya et al. 2004)]; (b) conditions close to (or beneath) the crust – mantle transition of the arc lithosphere (where high pressure fractionation of arc magmas is most likely); and (c) conditions of melting in the peridotitic mantle wedge (if adakites are generated by partial-melting of peridotite). Because adakites share similarities with rocks of the Archean tonalite-trodhjemite-granodiorite (TTG) series (see Martin et al. 2005), the conditions of their generation in the modern Earth also have implications for continental crust formation in the early Earth.

For these reasons, we have conducted an experimental study of an adakite from the Surigao peninsula in the Philippines, where adakitic rocks are prevalent (see Sajona et al. 1993; Macpherson et al. 2006). Originally, Sajona et al. (1993) postulated a slab melt origin

for the Surigao adakites, but subsequent investigations by Dreher et al. (2005) and Macpherson et al. (2006) favoured either: (a) high pressure fractionation of garnet ± amphibole from (normal) mafic arc magmas; or (b) partial melting of underplated arc basaltic rock, emplaced at sufficiently high pressure to crystallise garnet. Although garnet is not observed in any of the Surigao adakites, the distinctive chemistry of the adakites provides a cryptic signature of differentiation involving a garnet-bearing assemblage. Macpherson et al. (2008) used this factor to estimate that adakite magma generation occurred at depths >55 km.

Our study was conducted with the primary aim of testing the high-pressure fractionation model of Macpherson et al. (2006). Our approach was to examine the high pressure liquidus and sub-liquidus phase relations of the most primitive of the Surigao adakites (the basaltic andesite 357461) and to compare experimentally produced melt and mineral compositions with their natural Surigao equivalents.

Surigao adakitic magmatism, East Philippine Arc

The East Philippine Arc is associated with westward subduction of the Philippine Sea Plate beneath the Philippine archipelago (Figure 1). At its northern end, in southeast Luzon, the arc is fully mature but in its southern part in Surigao, northeastern Mindanao, subduction began more recently. Here, the East Philippine Arc has produced substantial quantities of adakitic magma. Thermal modelling, such as that by Peacock et al. (1994), indicates that the Philippine Sea Plate beneath Surigao is too cold to melt. Sajona et al. (1993) proposed that, because the convergent margin is itself quite young, the slab was entering unusually hot mantle and therefore could melt. However, Macpherson et al. (2006) showed that, excepting HREE and Y, adakitic and non-adakitic igneous rocks from Surigao display negligible contrasts in their trace element and isotopic characteristics. They therefore concluded that both types of magma were derived from the same mantle wedge source (Figure 3a and b in Macpherson et al. 2006). Furthermore, major and trace element variations indicate that the compositional variation observed at Surigao cannot be the product of magma mixing. The differences were suggested to be the result of adakitic Pliestocene magmas having experiencing an early, deep phase of garnet-present differentiation, which sequestered HREE and Y. This did not affect the non-adakitic Pliocene magmas, thereby creating different Sr/Y ratios in the Pleistocene and Pliocene magmas. High pressure fractionation during the Pleistocene is considered to have been produced either by high-pressure crystal fractionation

(within the garnet stability field), and/or during partial melting of a garnet-bearing rock (e.g. garnet amphibolite and/or amphibole-bearing eclogite) that had crystallised from normal arc basalt.

To explain the Surigao adakitic magmatism in the context of the developing East Philippine Arc, Macpherson (2008) proposed that beneath the mature arc in southeast Luzon convective flow in the mantle wedge has thinned the mantle lithosphere sufficiently to give basalt from the wedge unfettered access to the arc crust. Consequently, the petrologic and geochemical characteristics of magmatism in this mature arc segment are imposed by low-pressure differentiation in the crust. In contrast, there has been insufficient loss of mantle lithosphere beneath Surigao to prevent it from impeding the upward migration of basaltic magma generated in the wedge. High-pressure differentiation of this stalled magma produces the distinctive HREE- and Y-depletions that are characteristic of the Surigao adakites. These depletions are expressed by a strong increase in Dy/Yb with increasing SiO_2 (Figure 1).

Experimental and analytical procedures

Starting materials for experiments and natural samples studied for comparison:

A representative subset of Pleistocene adakite samples was used for mineral chemistry analysis and petrogenetic modelling. One sample, a basaltic andesite (357461, also termed SM61 here) was used as the experimental starting material. It is the most mafic (5.3% MgO) and least porphyritic of the Surigao adakites (Table 1). Three other samples (357430, 357433 and 357440) were chosen that seemed likely to be related by progressive crystal fractionation. Other samples included a non-adakitic dacite (357405) and a highly adakitic dacite (357417).

SM61 contains phenocrysts of amphibole (pargasitic hornblende and edenite) and plagioclase (An_{40}-An_{35}). Al-in-hornblende barometers (Hammarstrom and Zen 1986; Hollister et al. 1987; Schmidt 1992) suggest pargasite formation at 0.5-0.7 GPa with edenite formed later at 0.3-0.35 GPa. Crystallisation temperatures calculated using the formulation of Luhr et al. (1984) for rare unaltered biotites range from 992°C to 1042°C. Plagioclase phenocrysts show slight normal zoning, with most crystals showing calcic cores zoning to sodic rims. The temperature and pressure constraints provided a starting point for the experimental campaign which was designed to recreate near- and sub-liquidus conditions in

the original Surigao magmas. An aliquot of SM61 (used in runs 4 to 6) was also seeded with almandine garnet in order to overcome problems with nucleating garnet close to the low pressure limit of its stability. Almandine was chosen because it could be clearly distinguished from the more calcic and Mg-rich garnets produced by equilibrium growth during experiments.

Experimental methods:

A powder of sample 357461 was heated in a vertical drop furnace at 1400 °C for 4 hours and then quenched in water. The resulting glass was then powdered and re-melted a further two times before being checked for homogeneity and used in experiments. This glass is hereafter called SM61. Powdered SM61 was loaded into $Ag_{70}Pd_{30}$ capsules of approximately 4 mm length, with one end welded flat to enable close proximity to the thermocouple. Water was added to capsules with a graduated micro-syringe. Starting materials were thus provided with either 5 or 7.5 wt. % of distilled and deionised H_2O. The combined sample weight (H_2O + glass) in each capsule was 15 milligrams. While being sealed with a carbon arc weld, capsules were immersed in a water bath to avoid evaporation of the added H_2O. Each stage of the capsule making procedure was carefully checked by weighing. This included the reweighing of sealed capsules after they had been heated at 110 °C in an oven. This was done to test the watertight integrity of capsules. Any capsules that lost weight as a result of heating were discarded.

All experiments were conducted at Macquarie University, Australia, using a cold piston-in technique and an end-loaded piston cylinder apparatus of the type described by Boyd and England (1960). A minus 10 % correction for the effects of friction was applied to measured pressures (Green et al. 1966). Experimental pressures ranged from 0.5 to 2 GPa, and temperatures from 950 to 1150 °C. Furnace assemblies were of 1.27 mm diameter with air-fired boron-nitride inserts, Pyrex® inner sleeves and talc outer sleeves. Run 12, at 0.5 GPa was performed using a talc only sleeve to help maintain hydrostatic pressure prior to the achievement of final run temperature (it was found that Pyrex® sleeves were sufficiently strong at low temperatures to cause a low pressure shadow around sample capsules, which resulted in capsules rupturing and losing H_2O as heating commenced). Run temperatures were measured using W_3Re-$W_{25}Re$ thermocouples and automatically controlled to within ± 10 °C. Run temperatures were reached within 5 minutes of activating the furnaces. The

durations of experiments varied from 48 to 71 hours. Experiments were terminated by turning off power to the furnaces with quench rates of several hundred degrees in the first few seconds. Once extracted, capsules were cleaned, mounted in epoxy, longitudinally sectioned and then polished.

Electron microprobe

The major element compositions of experimental products were analysed using a Cameca SX100 Electron Microprobe housed in the GEMOC Geochemical Analysis Unit, Department of Earth Sciences, Macquarie University, Australia. Corrections to the raw data were made with the PAP program of Pouchou and Pichoir (1984). The accelerating voltage was 15 kV at a current of 20 nA. Counting times were 10 s for peaks and 5 s for each background. For minerals the beam was focussed at 1-2 µm whereas for glasses a beam diameter of 30 µm was used. Na_2O and K_2O were analysed first during each analytical cycle in order to minimise losses during analyses. The standards used were albite, orthoclase, kyanite, wollastonite, rutile, olivine, Mn-garnet and apatite. The precision of individual analyses is generally better than ± 0.1 wt. % although the variability of actual analyses was typically greater than this.

The homogeneity of crystals and glasses within each run was assessed by analysing phases a minimum of 10 times thus ensuring a broad spread of analyses across the capsule. One sigma standard deviations for analyses of minerals are <10 % of mean values whereas for glasses the deviation is only 2-3 %. Minor components such as Cr_2O_3 and NiO are the exceptions to this, as their low abundances bring them close to the detection limits of the instrument.

Results

Experiments:

A list of run conditions and products for successful experiments is presented in Table 2. Liquidus and sub-liquidus phase relationships derived from these data are plotted in Figure 2. Analyses of minerals and glasses (quenched melts) produced in individual experiments are given in Table 3. Most experiments were conducted with ~5 wt. % of added H_2O. This was the minimum concentration of dissolved H_2O required to stabilize amphibole in previous

experimental studies of andesitic and dacitic melts (e.g. Prouteau and Scalliet 2003). Two experiments were also conducted with ~7.5 wt. % of added H_2O.

Initial experiments were focused at temperatures ≥ 950 °C and pressures ≥ 1.5 GPa [consistent with the conditions of origin inferred by Macpherson et al. (2006)]. Under these conditions, and with 5 wt. % of H_2O added to the starting material, garnet is a near-liquidus phase and probable liquidus phase, together with clino- and orthopyroxene. At pressures < 1.5 GPa, orthopyroxene and clinopyroxene are the main near-liquidus phases. Olivine occurred as a sub-liquidus phase (together with amphibole and clinopyroxene) in only one experiment at 0.5 GPa and thus its stability appears to be confined to relatively low pressures. Amphibole is not a liquidus phase under any of the conditions examined in this study, but it is stable as a sub-liquidus phase at pressures up to 1.5 GPa and temperatures to at least 1050 ºC. The thermal maximum in amphibole stability appears to occur with about 5 wt. % H_2O added to the starting material (the concentration used in most of our experiments). Increasing the added H_2O to 7.5 wt. % decreased the stability of amphibole by ~100 ºC (Figure 2).

Although co-existing garnet and amphibole were not produced in any individual experiment, the reaction

amphibole = garnet + clinopyroxene + liquid (1)

is confined by the phase relationships to slightly above 1.5 GPa (see Figure 2). Along this boundary garnet and amphibole can co-exist as sub-liquidus phases.

Surigao mineral chemistry and petrography

Modes, whole rock compositions and analyses of representative phenocryst phases for the selected samples are listed in Table 1. All of the samples are strongly phyric with 10-15% of amphibole and 25-50% of plagioclase phenocrysts within a fine crystalline matrix. Some samples also contain a minor fraction of biotite phenocrysts. Sample 357433 (the most primitive of the Mt. Maniayao suite) contains clinopyroxene phenocrysts. Rare orthopyroxene is observed in lavas of similar composition, but these were not examined in this study.

Amphibole phenocryst compositions vary from pargasite to edenite (Figure 3), and tend to become more edenitic as their host rocks become more felsic. $^{[iv]}$Al versus $^{[M1-3]}$Ti (Figure 4) shows similar and extended variations for each of the Mt. Maniayao samples, whereas the non-adakitic basaltic andesite (sample 357405) is distinctive in having amphiboles with relatively little compositional variation and relatively low $^{[iv]}$Al and $^{[M1-3]}$Ti. Clinopyroxene phenocrysts are found in only one sample (357433), and are diopsidic (Figure 3).

Plagioclase phenocrysts are of predominantly andesine composition with reverse zoning in large crystals (e.g. average in 357433: An_{37} in core, An_{48} rims). Very large zoned crystals show sodic cores with greater Na content in mid zones, before grading into calcic rims. The most mafic of the Mt. Maniayao volcanic suite has plagioclase with An_{52}, while the most evolved sample from the suite has An_{35}. Sample 357430 contains oikocrystic plagioclase with An_{60}, as well as fragments of An_{40}.

Discussion

Phase relationships and high pressure fractionation

The experimental phase relations and run product compositions for SM61 can be used to test whether melts of adakitic andesite composition can be generated by high-pressure crystal fractionation from a more mafic parent (Table 4). Consistent with the petrogenetic model of Macpherson et al. (2006), the phase relations show that at pressures a little above 1.5 GPa and temperatures ≥ 1050 °C garnet is a liquidus phase of SM61. Although amphibole is not a liquidus phase under these conditions, it is potentially stable together with garnet as a sub-liquidus phase at temperatures ≤ 1050 °C.

In order to test whether more evolved adakite magmas could have been generated by garnet ± amphibole fractionation, or whether their major element characteristics represent a lower pressure differentiation stage, we used data from phases crystallised in experiments to model the removal of possible fractionating phases from mafic parent magma compositions (SM61 and 357433). The best-fitting result (lowest R^2 value) shows that the fractionating assemblage (cumulate) yields a good fit for major element compositions of more evolved Surigao adakites (≥ 61 wt. % SiO_2) through crystallisation of approximately equal proportions of amphibole and plagioclase, together with subordinate clinopyroxene (Table 4,

Figure 5). This demonstrates that late-stage magma processes strongly influenced major element distribution, which is consistent with the abundance of phenocryst phases in the Surigao rocks. These more silicic adakites are generally not consistent with direct formation by fractionation of garnet and amphibole from more primitive parents. This is because the principal compositional trends followed by the silicic adakites require the removal of a bulk cumulate that is more CaO- and SiO_2-rich than either just amphibole or garnet, i.e. plagioclase and clinopyroxene must also be involved (Table 4). The silicic adakites must, therefore, have already acquired a garnet signature for trace elements and REEs before the modelled fractionation at lower pressures that produced their major-elemental compositions. These results are consistent the findings of Martin (1987) who modelled similar compositional trends in Archaean TTGs from eastern Finland. The modelling here infers that removal of this low pressure cumulate may account for up to 50 % of the initial bulk magma volume. The low pressure fractionation model yields a poorer fit for in Surigao adakites with silica contents less than 61 wt. %, notably for Al_2O_3 (Figure 5). As these rocks do contain low pressure phenocrysts it is likely that differentiation in the crust has overprinted the compositions developed by crystallisation at deeper levels.

Comparison of natural and experimentally produced amphiboles and clinopyroxenes

Amphibole crystals were abundant in experimental runs performed at pressures ≤1.5 GPa, with these showing similar $^{[iv]}$Al and $^{[M1-3]}$Ti partitioning to the more felsic adakitic natural samples (357430, 357440, 357461, 357417; Figure 4). Experimental amphiboles do not replicate those in the non-adakitic sample (357405). The natural amphiboles in adakitic samples are slightly less silica-rich than experimental amphiboles (Figure 3), and have similar $^{[iv]}$Al and Ti partitioning (Figure 4) into their mineral structure. Figure 4 shows amphiboles were crystallised continuously during magma ascent, as the site volumes for T1 ($^{[iv]}$Al) and M3 (Ti) increase with decreasing pressure (Adam et al. 2007). Therefore, pressures of crystallisation for natural amphiboles were similar to slightly less than those used in experiments. Al-in-hornblende barometers (Hammarstrom and Zen 1986; Hollister et al. 1987; Schmidt 1992) yield crystallisation pressures for natural phenocrysts of 0.6 to 0.8 GPa in 357433, 0.6 to 1.0 GPa in 357430, and 0.6 to 0.7 GPa in the most felsic of the Mt. Maniayao suite (357440).

A similar comparison can be made for natural and experimentally produced clinopyroxenes. In experimental runs, these are generally less calcic than their natural

counterparts (Figure 3). However, the compositions of augites produced in low pressure experiments (≤ 1 GPa) are closer to those of the natural phenocrysts. Application of the clinopyroxene thermobarometer of Putirka et al. (2003) using groundmass as the liquid composition yields crystallisation conditions of 0.8 – 1.7 GPa and 980-1000 ºC, in broad agreement with the amphibole data. The petrographic, thermobarometic calculations and comparisons with experimental data are consistent with clinopyroxene commencing crystallisation first, then amphibole beginning ~0.8 – 1.0 GPa and both then continuing to precipitate as they ascended to lower pressures.

Constraining H_2O in the system

Although we did not conduct experiments with less than 5 wt. % of H_2O, previous studies (e.g. Scaillet and Evans 1999) have shown that at least 5 wt. % of dissolved H_2O is needed to stabilize amphibole in andesitic melts at temperatures much above 800 ºC. With this much H_2O in the starting composition amphibole is stable to at least 1050 ºC (Figure 2). But with 7.5 wt. % of H_2O the thermal stability of amphibole is reduced to ~950 ºC (at 1.5 GPa). A similar maximum in the thermal stability of amphibole at ~5 wt. % of dissolved H_2O was also noted by Eggler (1972) in his study of a Paricutin andesite. Calculated estimates for the crystallisation temperatures of the Surigao adakites are at least 1000 ºC (see previous section on rock chemistry and petrography). Thus the lower H_2O concentration of ~5 wt. % seems most consistent with the natural mineral data and is also close to previous estimates of H_2O concentrations in andesitic arc magmas and the mantle wedge (e.g. Rutherford and Devine 1988; Sisson and Grove 1993; Sisson and Layne 1993; Grove et al. 2003).

Development of Surigao adakitic magmatism

A principal aim of this study was to establish whether garnet could be a liquidus phase for Surigao adakitic rocks and, if so, to place firm constraints on the depth where this would be possible. Our experiments have demonstrated that garnet crystallises from SM61 containing 5 wt. % H_2O at pressures >1.5 GPa, which is equivalent to depths greater than 45 km. This is in good agreement with the estimate of Macpherson (2008) – based on Na contents and estimated crustal thickness in other arcs – that adakitic magma from Surigao crystallised at >55 km. Importantly, the minimum pressure derived from experiments strongly supports the contention that garnet fractionation took place within the mantle wedge, since gravity data suggests that the Surigao crust is no more than 29 km thick (Dimalanta and

Yumul 2003).

Amphibole and garnet are not co-liquidus phases of SM61 but could crystallise together at pressures close to 1.5GPa (Figure 2). However, the composition of much of the amphibole contained in the natural rocks suggests crystallisation at lower pressures. This discovery deviates from the model of Macpherson et al. (2006), who assumed that amphibole was part of the crystallising assemblage that produced the adakitic chemistry. Their work was based on experimental data for an unrelated basaltic composition (see Müntener et al. 2001). We are currently undertaking work to determine mineral/melt partition coefficients for SM61. This will help to provide a model for trace element evolution that is specific to Surigao magmatism.

Because the Mindanao adakites obtained their adakitic trace element signature prior to amphibole crystallisation, it is likely that they inherited this signature from a more primitive parent magmas (potentially SM61 and 357433) which did equilibrate with garnet. This could have occurred if the parent was produced by the partial-melting of garnet-bearing rocks (e.g. underplated eclogites and/or garnet-amphibolites). Alternatively, the parent magma could have undergone an initial high-pressure phase of crystal fractionation (at $\geq$1.5 GPa) that removed garnet, and then continued to evolve by crystal fractionation at lower pressures. This second option is consistent with the evidence of polybaric crystallisation described above for the amphibole phenocrysts. It is also consistent with Macpherson et al.'s (2006) model and provides a similar explanation for the specific compositional differences, confined essentially to Y and HREE concentrations, between adakitic and non-adakitic volcanics from Mount Mindanao.

We suggest a model of magma generation and development that can be traced over at least three stages (Figure 6). During stage 1 the peridotitic mantle wedge beneath Surigao was fluxed by H_2O-fluids from the subducting Philippine Sea Plate. Because of the steeply dipping nature of the plate (Acharya and Aggarwal 1980; Cardwell 1980), the mantle beneath the Surigao Peninsula received continuous H_2O input (Schmidt and Poli 1998). During stage 2 melts produced by fluxing of the mantle wedge ascended and then stalled at the base of a 45-60 km thick lithosphere where they began to cool and crystallise a high-pressure cumulate assemblage, which included garnet. During stage 3, residual magma ascended to shallower

(i.e. crustal) depths and crystallized their main phenocryst assemblage which is dominated by amphibole and plagioclase.

A similar petrogenetic model was developed for the 1991 Pinatubo dacites to the north in Luzon (Prouteau and Scaillet 2003). Experimental interaction experiments demonstrated that melting of subducted oceanic lithosphere and interaction of the resulting melts with peridotite would not produce adakitic melts. Instead, Prouteau and Scaillet (2003) showed that the crystallisation of garnet during cooling of a hydrous and oxidised, basaltic melt could have caused HREE depletions in these recent volcanic sequences. Interestingly, some interstitial melt compositions in harzburgitic xenoliths from the northern Philippines are comparable to SM61 (see Arai et al. 2004) supporting the view that such melts could have been produced in the mantle wedge beneath Mindanao.

Although garnet has not been found in any of the Surigao adakites, this is consistent with the relatively high density of garnet and polybaric fractionation to relatively low pressures. The occurrence of cognate garnet-bearing cumulates and megacrysts in arc-related New Zealand dacites (Day et al. 1992; Green and Day 1992) is evidence that such high-pressure fractionation of arc magmas does, in fact, occur.

Two alternatives to the high pressure crystal-fractionation model are: (a) partial-melting of underplated arc basalts, and (b) partial melting of garnet-bearing wedge peridotites (see Macpherson et al. 2006; Eiler et al. 2007). With regard to the first alternative, our experiments with 5 wt. % H_2O constrain garnet fractionation to pressures beneath the current sub-Surigao Moho. But as emphasized by Alonso-Perez et al. (2009) higher magmatic H_2O concentrations (and thus lower liquidus temperatures) would allow garnet to be stabilized at shallower depths. However, estimated crystallisation temperatures for the adakites favour the original estimate of 5 wt. % of magmatic H_2O. It is also easier to explain the similar geochemistry of adakitic and non-adakitic Surigao andesites (excluding their Y and HREE concentrations) if both formed by essentially similar processes. The case against alternative (b) is that peridotite melting under the conditions required to stabilize garnet produces melts that are both mafic and SiO_2-poor (see Green 1989 and references therein). Thus these melts are typically either basanitic or nephelinitic. Such highly alkaline melts would be unlikely to evolve into the quartz normative andesites that are characteristic of the Surigao Peninsula.

Conclusions

Our experiments provide broad support for the petrogenetic model of Macpherson et al. (2006) for adakitic volcanics in Mindanao. Thus, at pressures close to 1.5 GPa and temperatures > 1050 ºC garnet, clinopyroxene and orthopyroxene are either liquidus or near-liquidus phases of the most primitive adakite sampled (the basaltic andesite SM61). However, the original model needs to be modified to include a role for post-garnet crystallisation of amphibole and plagioclase. This is because amphibole is not a liquidus phase of the most primitive adakites, and the principle fractionation trends of the adakites require crystal fractionation involving both amphibole and plagioclase.

Our results provide support for the contention that adakitic melts need not be generated by the melting of subducted ocean crust, but that they are instead generated by essentially normal arc processes.

Acknowledgements

B. Coldwell and T. Rushmer acknowledge the support of DP0986232 to T. Rushmer. C. Macpherson acknowledges support from the Southeast Asia Research Group of the University of London. B. Coldwell would also like to thank Norm Pearson for analytical support. This is contribution 708 from the Australian Research Council National Key Centre for the Geochemical Evolution and Metallogeny of Continents (http://www.gemoc.mq.edu.au). The analytical data were obtained using instrumentation funded by ARC LIEF, and DEST, Systemic Infrastructure Grants, industry partners and Macquarie University. We thank two anonymous reviewers for their constructive criticisms of this manuscript.

References

Adam J, Oberti R, Camara F (2007) An electron microprobe, LAM-ICP-MS and single-crystal X-ray structure refinement study of the effects of pressure, melt-H_2O concentration and fO_2 on experimentally produced basaltic amphiboles. Eur J Mineral 19(5):642-655

Alonso-Perez R, Müntener O, Ulmer P (2009) Igneous garnet and amphibole fractionation in the roots of island arcs: experimental constraints on andesitic liquids. Contrib Mineral Petrol 157(4):541-558

Acharya HK, Aggarwal YP (1980) Seismicity and tectonics of the Philippine islands. J Geophys Res 85:3239-3250

Arai S, Takada S, Michibayashi K, Kida M (2004) Petrology of peridotite xenoliths from Iraya volcano, Philippines, and its implication for dynamic mantle-wedge processes. J Petrol 45:369-389

Atherton MP, Petford N (1993) Generation of sodium-rich magmas from newly underplated basaltic crust. Nat 362:144-146

Boyd FR, Englad JL (1960) Apparatus for phase-equilibrium measurements at pressures up to 50 kilobars and temperatures up to 1750 °C. J Geophys Res 65:741-748

Cardwell R, Isacks B, Karig D (1980) The spatial distribution of earthquakes, focal mechanism solutions, and subducted lithosphere in the Philippines and northeast Indonesian islands. In: Hayes DE (ed) The Tectonic and Geologic Evolution of Southeast Asian Seas and Islands, Part 1. AGU Geophys Monogr 23:1-35

Castillo PR, Janney PE, Solidum RU (1999) Petrology and geochemistry of Camiguin Island, southern Philippines: insights to the source of adakites and other lavas in a complex arc setting. Contrib Mineral Petrol 134:33–51

Chiaradia M, Fontbote L, Beate B (2004) Cenozoic continental arc magmatism and associated mineralization in Ecuador. Miner Depos 39:204–222

Day RA, Green TH, Smith IEM (1992) The origin and significance of garnet phenocrysts and garnet-bearing xenoliths in Miocene calc-alkaline volcanics from Northland, New Zealand. J Petrol 33: 125-161

Defant MJ, Drummond MS (1990) Derivation of some modern arc magmas by melting of young subducted lithosphere. Nat 347(6294):662-665

Dimalanta CB, Yumul GP (2003) Magmatic and amagmatic contributions to crustal growth of an island-arc system: The Philippine example. Int Geol Rev 45:922–935

Dimalanta CB, Yumul GP (2004) Crustal thickening in an active margin setting (Philippines): The whys and the hows. Episodes 27(4)

Dreher ST, Macpherson CG, Pearson DG, Davidson JP (2005) Re-Os isotope studies of Mindanao adakites: Implications for source metals and melts. Geol 33:957–960

Eggler DH (1972) Water-saturated and undersaturated melting relations in a Paricutin andesite and an estimate of water content in the natural magma. Contrib Mineral Petrol 34:261-271

Eiler JM, Schiano P, Valley JW, Kita NT, Stolper EM (2007) Oxygen-isotope and trace element constraints on the origins of silica-rich melts in the mantle. Geochem Geophys Geosystems 8:Q09012

Garrison JM, Davidson JP (2003) Dubious case for slab melting in the Northern volcanic zone of the Andes. Geol 31(6):565-568

Gerya TV, Yuen DA, Sevre EOD (2004) Dynamical causes for incipient magma chambers above slabs. Geol 32:89-92

Green DH (1989) Experimental petrology. In: Johnson RW (ed) Intraplate volcanism in eastern Australia and New Zealand. Cambridge University Press, Cambridge, pp 321-324

Green TH, Ringwood AE, Major A (1966) Friction effects and pressure calibration in a piston-cylinder apparatus at high-pressure and temperature. J Geophys Res 71:3589-3594

Green TH, Day RA (1992) Experimental phase equilibria studies of garnet-bearing I-type volcanics and high-level intrusives from Northland, New Zealand. Trans R Soc Edinburgh Earth Sciences 83:429-438

Grove TL, Elkins-Tanton LT, Parman SW, Chatterjee N, Müntener O, Gaetani GA (2003) Fractional crystallisation and mantle-melting controls on calc-alkaline differentiation trends. Contrib Mineral Petrol 145:515–533

Hammarstrom JM, Zen E-an (1986) Aluminum in hornblende; an empirical igneous geobarometer. American Mineral 71(11-12):1297-1313

Hollister LS, Grissom GC, Peters EK, Stowell HH, Sisson VB (1987) Confirmation of the empirical correlation of Al in hornblende with pressure of solidification of calc-alkaline plutons. American Mineral 72:231-239

Luhr JF, Carmichael IEE, Varekamp JC (1984) The 1982 eruption of El Chichon volcano, Chipas, Mexico: Mineralogy and petrology of the anhydrite-bearing pumices. J Volcanol Geotherm Res 23:69-108

Macpherson CG, Dreher ST, Thirlwall MF (2006) Adakites without slab melting: High pressure processing of basaltic island arc magma, Mindanao, the Philippines. Earth Planet Sci Lett 243:581–593

Macpherson CG (2008) Lithosphere erosion and crustal growth in subduction zones: Insights from initiation of the nascent East Philippine Arc. Geol 36:311-314

Martin H (1987) Petrogenesis of Archaean trondhjemites, tonalites and granodiorites from Eastern Finland: major and trace element geochemistry. J Petrol 28: 921-954

Martin H, Smithies RH, Rapp R, Moyen J-F, Champion D (2005) An overview of adakite, tonalite-trondhjemite-granodiorite (TTG), and sanukitoid: relationships and some implications for crustal evolution. Lithos 79:1-24

Müntener O, Kelemen PB, Grove TL (2001) The role of H_2O during crystallization of primitive arc magmas under uppermost mantle conditions and genesis of igneous pyroxenites: An experimental study. Contrib Mineral Petrol 141:643–658

Peacock SM, Rushmer T, Thompson AB (1994) Partial melting of subducting oceanic crust.

Earth Planet Sci Lett 121:227-244

Pouchou JL, Pichoir F (1984) A new model for quatitative X-ray microanalysis, Part II: Application to in-depth analysis of heterogeneous samples. Rech Aerosp 1984-5:47-65

Prouteau G, Scaillet B (2003) Experimental constraints on the origin of the 1991 Pinatubo dacite. J Petrol 44:2203–2241

Putirka KD, Mikaelian H, Ryerson F, Shaw H (2003) New clinopyroxene-liquid thermobarometers for mafic, evolved, and volatile-bearing lava compositions, with applications to lavas from Tibet and the Snake River Plain, Idaho. American Mineral 88:1542–1554

Rutherford M J, Devine JD (1988) The May 18, 1980, eruption of Mount St. Helens, 3. Stability and chemistry of amphibole in the magma chamber. J Geophys Res 93:11949-11959

Sajona FG, Maury RC, Bellon H, Cotton J, Defant MJ, Pubellier M (1993) Initiation of subduction and the generation of slab melts in western and eastern Mindanao, Philippines. Geol 21:1007-1110

Scaillet B, Evans B (1999) The June 15, 1991 eruption of Mount Pinatubo. I. Phase equilibria and pre-eruption P-T-fO2-fH2O conditions of the dacite magma. J Petrol 40:381-411

Schmidt MW (1992) Amphibole composition in tonalite as a function of pressure: an experimental calibration of the Al-in-hornblende barometer. Contrib Mineral Petrol 110:304-310

Schmidt MW, Poli S (1998) Experimentally based water budgets for dehydrating slabs and consequences for arc magma generation. Earth Planet Sci Lett 163:361-379

Sisson TW, Grove TL (1993) Experimental investigations of the role of H_2O in calc-alkaline differentiation and subduction zone magmatism. Contrib Mineral Petrol 113:143-166

Sisson TW and Layne GD (1993) H_2O in basalt and basaltic andesite glass inclusions from four subduction related volcanoes. Earth Planet Sci Lett 117:619-635

Tulloch AJ, Kimbrough DL (2003) Paired plutonic belts in convergent margin and the

development of high Sr/Y magmatism: The Peninsular Ranges Batholith of California and the Median Batholith of New Zealand. Geol Soc America Special Paper 374

FIGURE CAPTIONS

Fig. 1 a) Map of the Philippines and location of Surigao. PF: Philippine Fault. b) Dy/Yb vs. SiO_2 for samples from Mindanao presented in Macpherson et al. (2006). This shows garnet influence directly related to fractionation

Fig. 2 Phase diagram detailing the relationships between minerals at varying run conditions using SM61 as a start material with 5 wt. % H_2O. Grey lines and symbols are experiments conducted at 7.5 wt% H_2O

Fig. 3 a) Si versus $Mg/(Mg + Fe^{2+})$ classification of amphibole. Grey shaded field shows range of experimental products. b) Clinopyroxene classification, with those formed in higher pressure experiments (≥1.5 GPa) as the grey shaded field. Experimental clinopyroxenes are less calcic than natural ones, likely due to their equilibrated state with either amphibole or garnet. Low pressure experimental clinopyroxenes lie closest to those in the Surigao rocks , suggesting these may be derived from similar conditions

Fig. 4 $^{[iv]}Al$ vs. $^{[M1-3]}Ti$ a.p.f.u for amphiboles in the selected natural samples (Table 1). The shaded field represents amphiboles formed in experiments

Fig. 5 Fractionation and removal of cumulates represented on major-element oxide versus SiO_2 diagrams. M = [MgO+FeO]*[40.32/71.85] + MnO*[40.32/70.94]. The trends in adakitic andesites from the Mindanao region (Supplementary Data from Macpherson et al. 2006) can be back-projected to a bulk cumulate (solid square) composed of 21 % amphibole, 23 % plagioclase and 6 % clinopyroxene (Table 4), i.e. this assemblage was removed from a more mafic parent.

Fig. 6 Present-day tectonic configuration of the Mindanao section of the Philippine subduction system (9-10° N) after Acharya and Aggarwal (1980); Dimalanta and Yumal (2003; 2004); Macpherson (2008). Dashed diagonal lines indicate the area investigated by experiments. The Philippine Sea Plate, when it began subducting between 5-7 Ma, was ~50 Ma. When the Surigao adakitic volcanics were erupted in the Pleistocene, the Philippine crust was thick enough to cause magmas derived from the mantle wedge (No. 1) to stall beneath thick lithosphere (No. 2). Here they crystallised garnet, orthopyroxene and clinopyroxene, before liquids were able to move upwards (No. 3) where they could crystallise amphibole, plagioclase plus clinopyroxene. Present-day, well-developed corner flow in the mantle wedge has caused lithospheric erosion and thinning of the crust, so that magmas now stall at higher levels and stage 1 does not occur (Macpherson 2008)

colour figure

Click here to download colour figure: Fig 1 Map and DyYb.eps

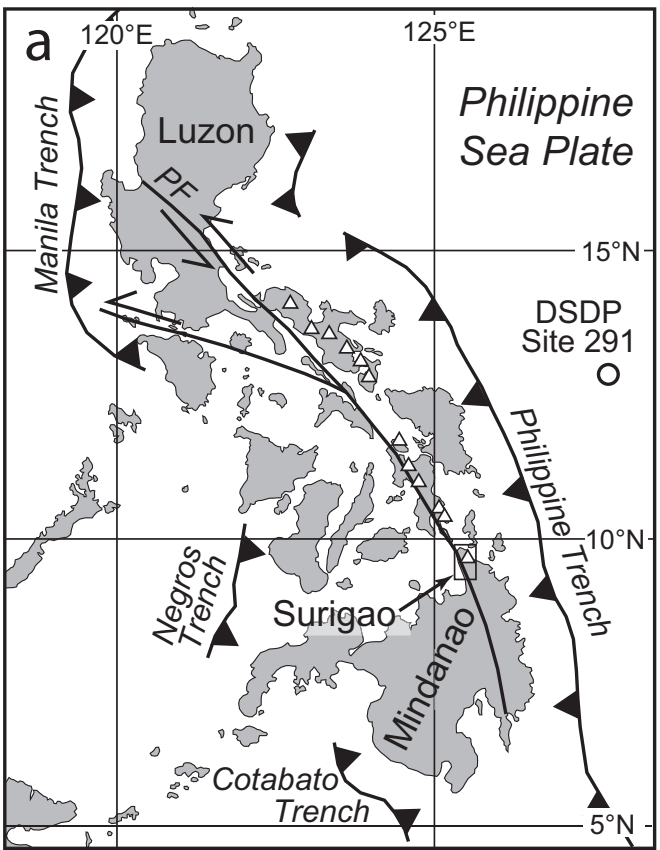

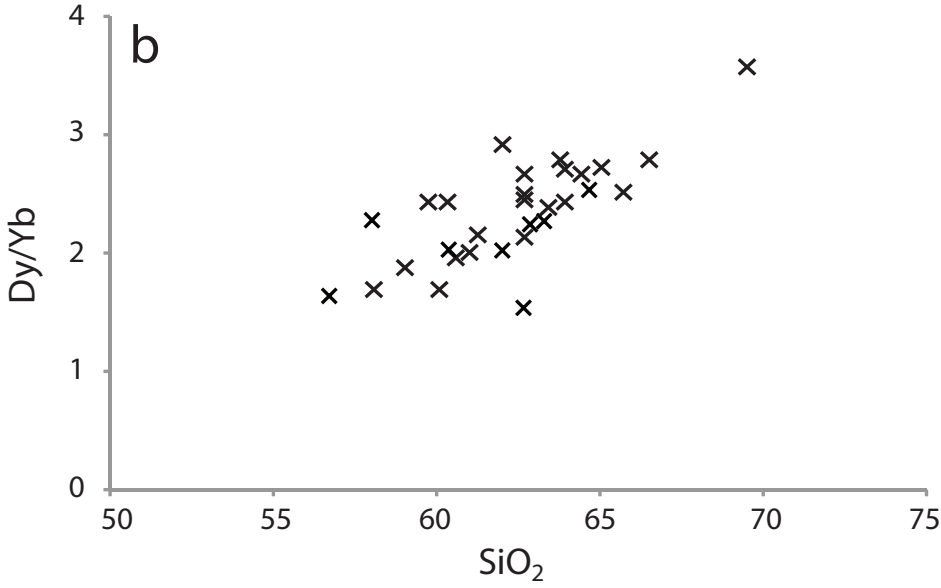

colour figure

Click here to download colour figure: Fig 2 Phase relations.eps

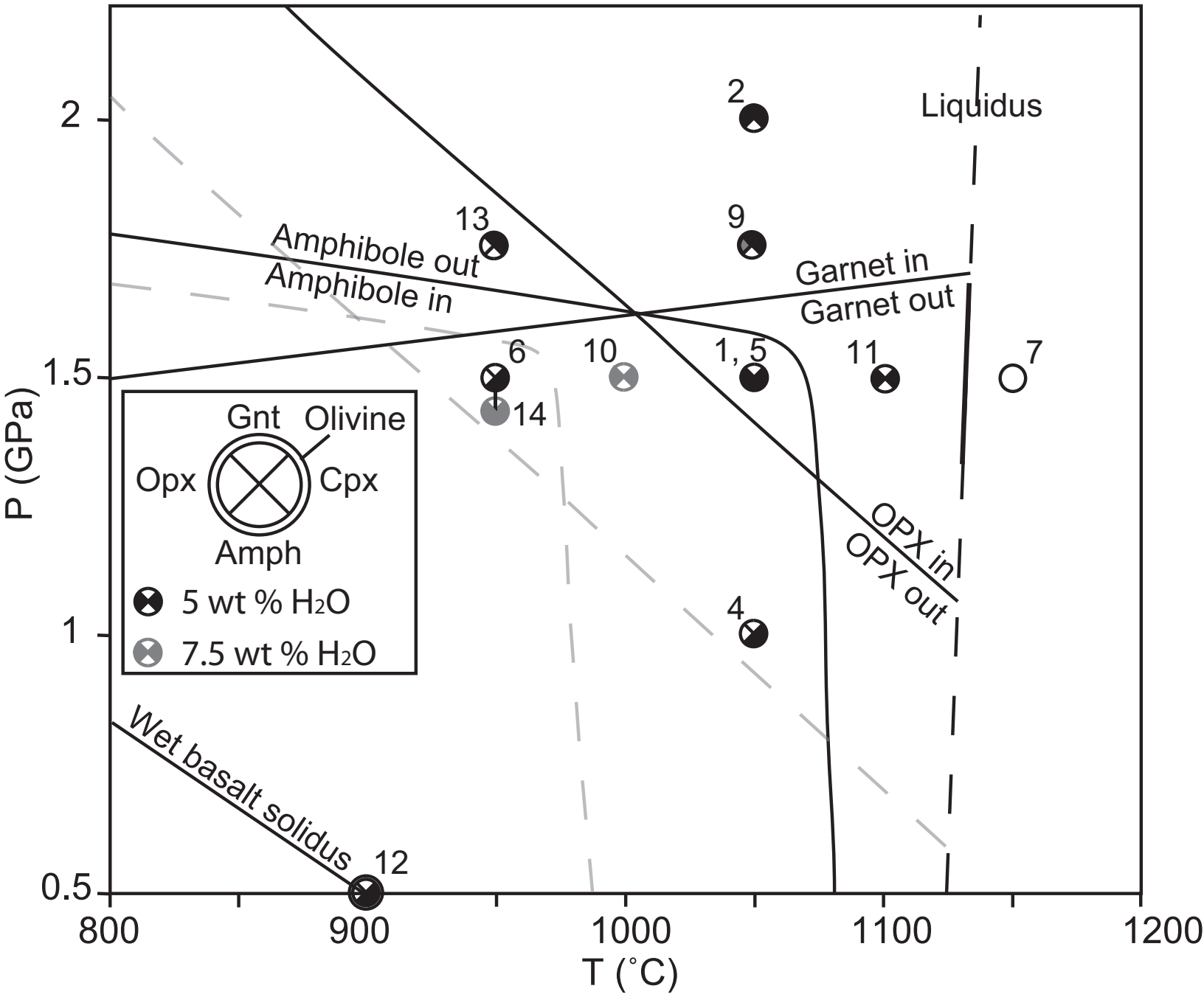

colour figure
Click here to download colour figure: Fig 3 pheno comps nat+exp.eps

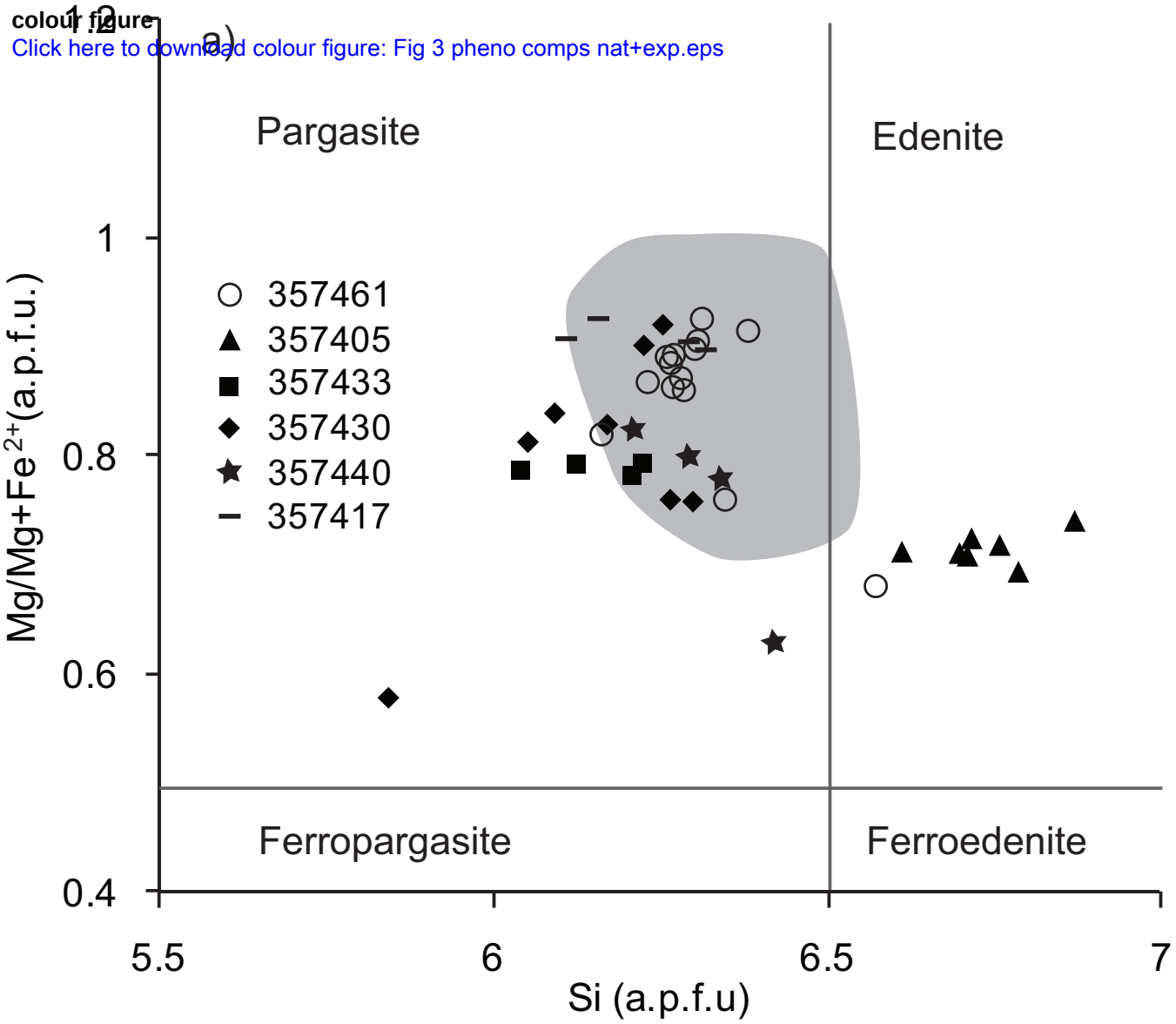

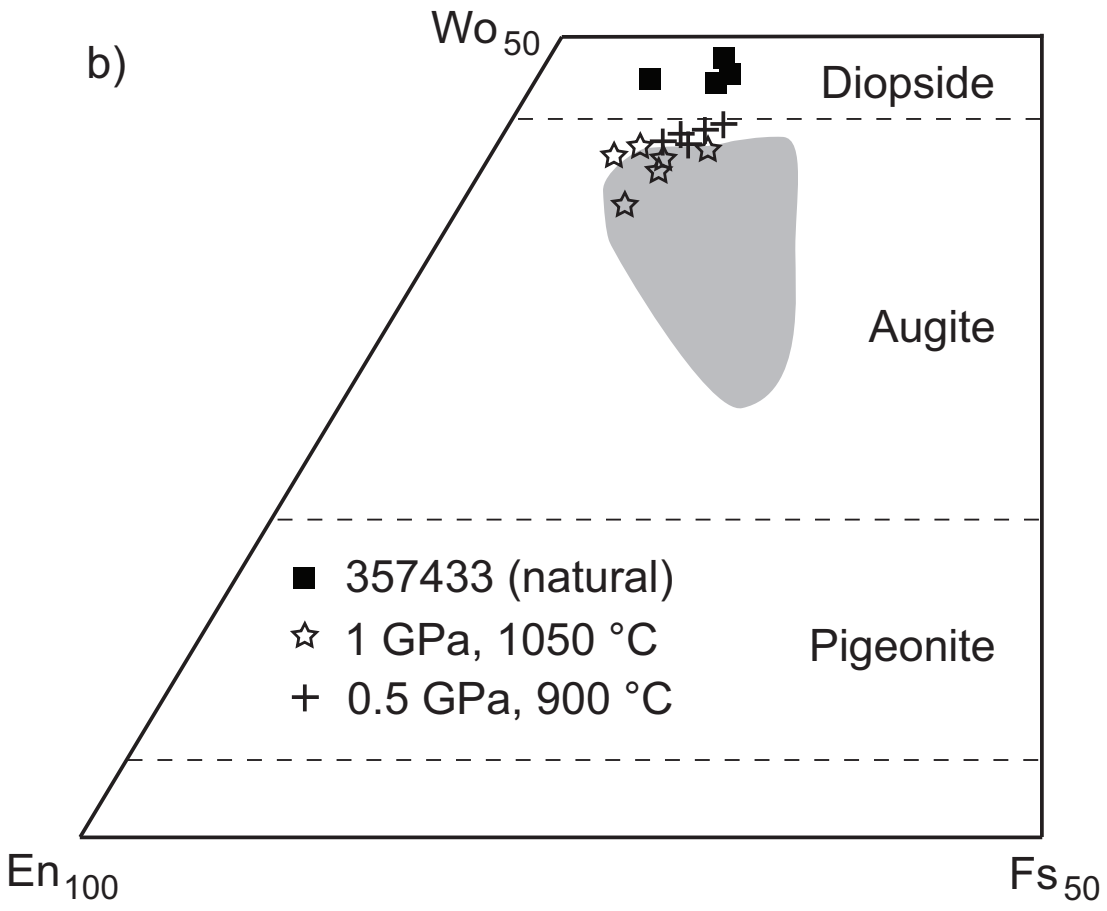

colour figure

Click here to download colour figure: Fig 4 Amph pressure partitioning.eps

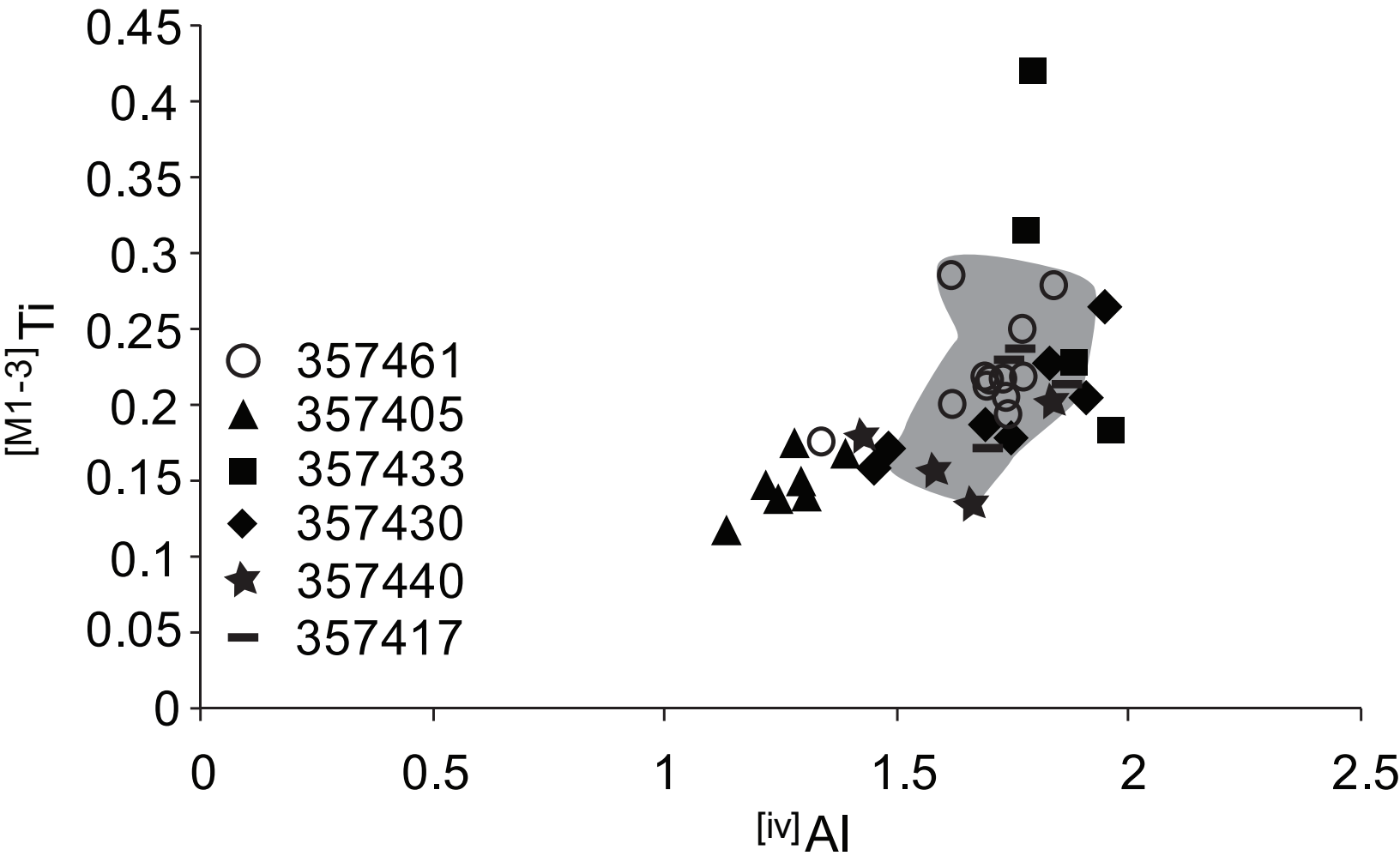

colour figure

Click here to download colour figure: Fig 5 cumulate removal.eps

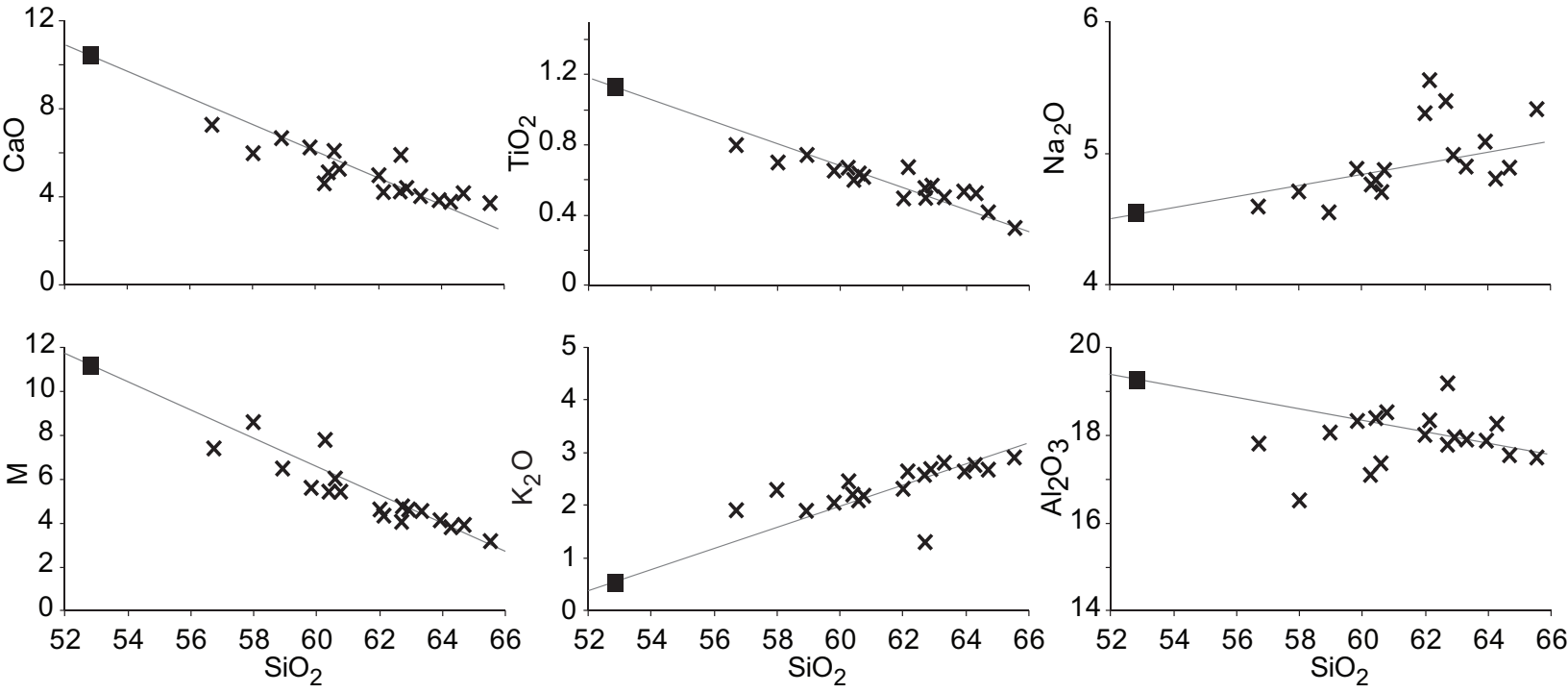

colour figure

Click here to download colour figure: Fig 6 Mindanao configuration.eps

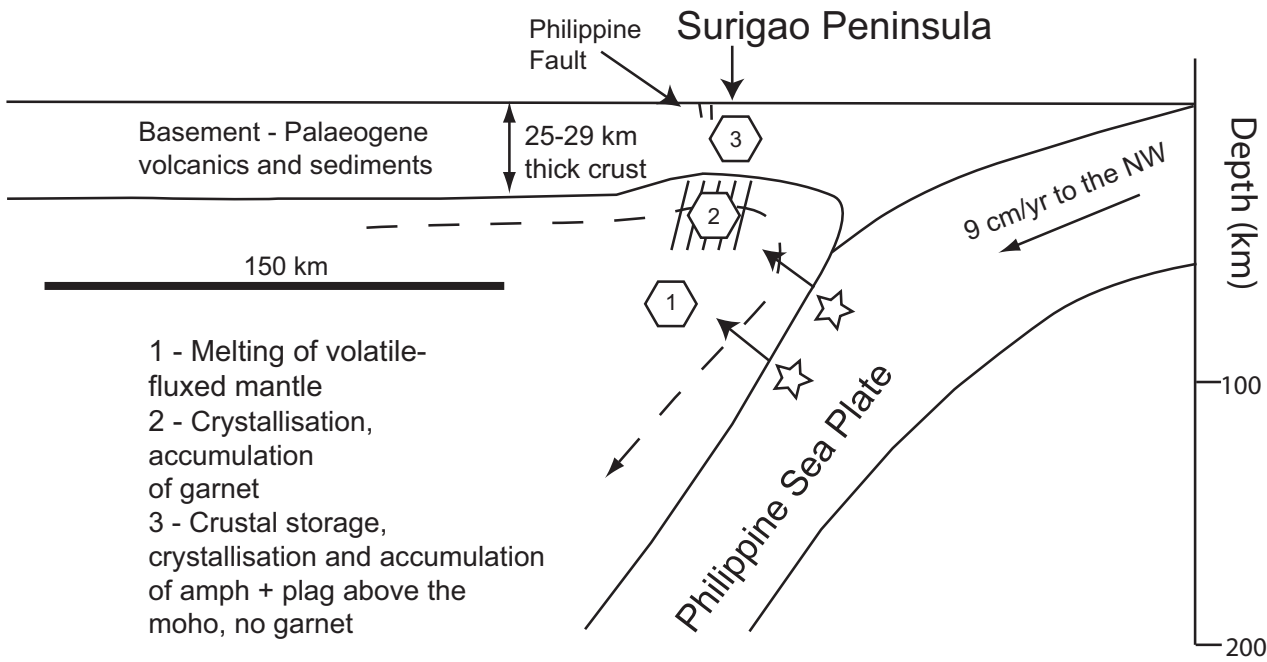

table

Click here to download table: Table 1 Natural rocks and phenocrysts.xls

Table 1 A) Geochemical data from selected samples from the Macpherson et al. (2006) suite, five adakitic and one non-adakitic. Major and trace elements analysed by XRF; REE analysed by ICP-MS (Macpherson et al. 2006). Phenocryst modes given by the average of two counts of 400 points, then renormalized to 100%. Mg# calculated as Mg# = 100*(mol Mg/[mol Mg+mol Fe]), with FeO as total Fe. B) Average phenocryst compositions from 10 analyses of the major phases present in samples from Table 1A. Analyses performed by electron microprobe at Macquarie University (see Analytical Details section for details).

1A Whole rock

Sample	357405	357430	357433	357440	357461	357417
SiO_2	62.7	62	56.7	60.4	58	63.3
TiO_2	0.5	0.5	0.8	0.6	0.7	0.5
Al_2O_3	19.2	18	17.8	18.4	16.5	17.9
Cr_2O_3	-	-	-	-	-	-
Fe_2O_3	5.2	4.2	6.4	5.1	5.8	4.2
MnO	0.1	0.1	0.1	0.1	0.1	0
MgO	1.1	2.2	3.8	2.5	5.3	2.2
CaO	5.9	5	7.3	5.1	6	4
Na_2O	3.9	5.3	4.6	4.8	4.7	4.9
K_2O	1.3	2.3	1.9	2.2	2.3	2.8
NiO	-	-	-	-	-	-
P_2O_5	0.2	0.2	0.3	0.2	0.3	0.2
LOI	1	0.2	0.3	0.6	0.8	1.2
Total	100.2	100	100	99.7	100.1	100.3
Mg#	32.3	54.6	57.6	53.6	68	55.4
Sc	13.1	9.6	16.3	11	13	10.6
V	109.6	133.1	222.1	147.2	142.7	91.1
Cr	8.7	24.9	40.2	38.2	230.5	157.9
Ni	6.7	12.1	27.1	48.5	124.4	45.4
Cu	22.4	18.5	58.4	45.9	58.9	52.5
Zn	61.8	57.2	64.9	62.6	70.5	58
Ga	19.7	23.7	21.7	23	21.6	21.1
Rb	26.5	41.8	29.1	40.7	41.6	55.6
Sr	534.5	914.8	860	874.7	968.8	957.2
Y	16	10.2	15.4	11.2	11.3	9.2
Zr	94.3	119	98.7	111.9	120.4	129.3
Nb	3.1	4	2.7	3.9	7.3	4.2
Ba	351.2	462.8	344.9	480.3	526.3	567
Nd	9.6	13.8	16.3	13.5	16.7	16.2
Pb	4.5	9.3	7.2	9.4	8.4	14
Th	0.4	2.6	1.8	1.9	1.5	2.1
Sr/Y	33.4	89.7	55.8	78.1	85.7	104.0
La	7.9	14.2	12.9	15.6	15.2	14.3
Ce	15.1	28	27	31.6	30	22.3
Pr	2.3	3.7	3.9	3.6	4.3	3.9
Nd	9.9	15	16.6	14.5	17.8	15.9
Sm	2.3	2.8	3.4	2.9	3.5	3
Eu	0.8	0.8	1	0.9	1	0.9
Gd	2.5	2.2	3.1	2.4	2.9	2.4
Tb	0.4	0.3	0.4	0.3	0.4	0.3
Dy	2.4	1.6	2.5	1.8	2	1.5
Ho	0.5	0.3	0.5	0.4	0.4	0.3
Er	1.4	0.8	1.4	0.9	0.9	0.7
Tm	0.2	0.1	0.2	0.1	0.1	0.1
Yb	1.5	0.8	1.5	0.9	0.9	0.7
Lu	0.3	0.1	0.3	0.1	0.1	0.1
Hf	1.8	2.1	2.6	1.7	2.2	2.5
Ta	0.2	0.3	0.2	0.2	0.5	0.3
U	0.6	1.2	0.9	0.9	0.9	1.4
Plagioclase	47.8	30.5	33.3	25.6	15.3	28.4
Amphibole	7.4	14.6	15.3	16.2	9.6	14.7
Quartz	0	0	0	0	0	0
Clinopyroxene	0	0	6.4	0	0	0
Biotite	0	1.5	0.4	0	1.3	2
Apatite	0	0.6	0	0.2	0	1.6
Oxides	1.8	2.1	1.6	1.2	0.6	1.8
Groundmass	43	50.7	43	56.8	73.2	51.5
Total	100	100	100	100	100	100

1B Average phenocryst composition

	357405		357430			357433			
	Amph	Plag	Amph	Plag	Bt	Amph	Plag	Cpx	Bt
SiO_2	46.37	56.67	43.30	59.14	37.35	41.71	57.04	51.22	37.16
TiO_2	1.36	0.01	1.83	0.01	3.62	2.51	0.02	0.53	3.75
Al_2O_3	8.34	26.70	11.46	25.26	14.00	12.31	26.05	3.04	13.95
Cr_2O_3	0.01	0.00	0.04	0.00	0.03	0.01	0.01	0.08	0.02
FeO	15.32	0.28	11.87	0.19	18.03	11.31	0.42	7.26	16.80
MnO	0.62	0.01	0.25	0.01	0.26	0.16	0.02	0.28	0.28
MgO	12.70	0.00	14.28	0.00	13.01	14.02	0.00	14.43	13.96
CaO	11.39	9.83	11.70	7.62	0.14	11.68	9.10	22.52	0.17
Na_2O	1.48	5.79	2.38	6.78	0.42	2.57	5.97	0.44	0.42
K_2O	0.45	0.21	0.79	0.34	8.83	0.74	0.45	0.01	8.85
NiO	0.01	0.01	0.01	0.01	0.02	0.01	0.01	0.00	0.02
Total	98.06	99.50	97.92	99.36	95.73	97.04	99.08	99.81	95.38
Mg#	59.62	-	68.20	-	-	68.84	-	77.97	-

	357440		357461			357417		
	Amph	Plag	Amph	Plag	Bt	Amph	Plag	Bt
SiO_2	43.67	60.45	44.36	61.01	37.76	43.17	62.77	36.93
TiO_2	1.52	0.01	1.91	0.01	3.87	1.87	0.00	3.37
Al_2O_3	11.69	24.57	10.87	24.07	13.96	12.35	22.49	14.05
Cr_2O_3	0.15	0.01	0.08	0.01	0.02	0.03	0.00	0.04
FeO	13.45	0.17	10.87	0.18	16.79	8.10	0.17	19.27
MnO	0.32	0.01	0.23	0.01	0.22	0.07	0.01	0.30
MgO	12.68	0.00	14.91	0.00	13.90	16.44	0.00	12.12
CaO	11.58	6.71	11.50	6.20	0.20	11.75	4.42	0.09
Na_2O	2.26	7.15	2.56	7.48	0.46	2.50	7.99	0.39
K_2O	0.91	0.42	0.89	0.55	8.81	1.00	0.85	8.86
NiO	0.03	0.01	0.04	0.01	0.03	0.02	0.01	0.01
Total	98.26	99.51	98.22	99.52	96.03	97.31	98.70	95.42
Mg#	62.69	-	70.96	-	-	78.34	-	-

table

Click here to download table: Table 2 Run conditions and products.xls

Table 2 Piston-cylinder run conditions and products. Modes derived from least squares mass balance calculations (Albaréde 1995), with low $\sum r^2$ showing glasses have analysed correctly and major phases are accounted for. Amphibole, as a hydrous phase, has 2 % water within its structure and is therefore accounted for in mass balance. Any Fe loss to the capsule or Na loss to the beam has also been corrected for in these calculations. Experiments 3 and 13 experienced water loss and quench crystallisation, respectively, therefore they are included here as indicators of those P and T conditions only. Where a phase was too small to gain accurate analyses but present in the charge, the mode is given in brackets.

Run	Sample mass (g)	H_2O (g)	H_2O (wt. %)	T (°C)	P (GPa)	Duration (hrs)	Products	Modes (mass balanced)	$\sum r^2$
1	0.01432	0.00077	5.1	1050	1.5	71	amph, cpx, opx,gl	7.3, 13, 2.2, 77.5	0.28
2	0.01425	0.00075	5	1050	2	68	gnt, cpx, opx,gl	7, 20, 1.5, 71.5	0.21
3	0.01427	0.00074	4.9	1150	1.5	50	plag, cpx, opx, gl	1.5, 17, 1.9, 79.6	0.28
4	0.01428	0.00077	5.1	1050	1	48	amph, cpx, gl	30, 3.8, 66.2	0.14
5	0.01425	0.00076	5	1050	1.5	56	amph, cpx, opx, gl	5, 11, 1.5, 82.5	0.18
6	0.01422	0.00074	4.9	950	1.5	60	amph, cpx, gl	28.5, 1, 70.5	0.2
7	0.01425	0.00073	4.9	1150	1.5	51	glass	100	-
9	0.01428	0.00075	5	1050	1.75	66	gnt, cpx, gl (opx)	0.1, 13, 82.9 (4)	0.3
10	0.01385	0.00114	7.6	1000	1.5	64	cpx, opx, gl	7, 3, 90	0.35
11	0.01421	0.00078	5.2	1100	1.5	58	cpx, opx, gl	10, 2, 83	0.02
12	0.01422	0.00073	4.9	900	0.5	68	amph, ol, cpx, gl	3.5, 3.5, 8.5, 84.5	0.12
13	0.01428	0.00077	5.1	950	1.75	49	gnt, cpx, gl	0.4, 18, 81.6	0.45
14	0.01385	0.00116	7.7	950	1.5	70	cpx, opx, amph, gl	9, 2, 3, 86	0.21

table

Click here to download table: Table 3 Experimental glass and mineral compositions.xls

Table 3 Melt (glass) and mineral compositions from experimental runs, analysed by EMP at Macquarie University. Glasses are given on an anhydrous basis, with hydrous totals also displayed

	Glass													
Experiment	**SM61**	**1**	**2**	**3**	**4**	**5**	**6**	**7**	**9**	**10**	**11**	**12**	**13**	**14**
***n*=**	*20*	*20*	*20*	*20*	*20*	*20*	*20*	*20*	*20*	*20*	*20*	*20*	*20*	*20*
SiO_2	58.91	61.08	63.39	60.63	64.80	59.22	63.17	58.76	59.69	58.80	59.63	61.22	59.28	59.91
TiO_2	0.80	0.83	0.84	0.85	0.20	0.83	0.41	0.82	0.85	0.86	0.83	0.71	0.64	0.86
Al_2O_3	16.06	18.93	18.39	18.44	18.35	18.68	18.30	16.72	18.73	18.19	17.60	18.31	17.50	18.38
Cr_2O_3	0.00	0.00	0.00	0.01	0.01	0.01	0.01	0.00	0.01	0.01	0.01	0.01	0.03	0.01
FeO	5.17	4.28	3.26	4.85	3.68	5.56	4.37	5.24	4.86	5.17	5.02	4.28	4.35	4.83
MnO	0.10	0.06	0.03	0.06	0.08	0.07	0.08	0.08	0.07	0.08	0.08	0.08	0.05	0.06
MgO	5.32	2.16	1.77	2.55	0.53	2.88	1.39	4.88	2.56	3.53	3.57	2.33	3.95	2.97
CaO	6.05	3.67	2.85	3.91	3.35	4.63	3.74	5.64	4.35	5.22	4.82	4.36	5.99	4.32
Na_2O	4.86	5.71	6.18	5.43	5.78	5.15	5.41	5.14	5.73	5.28	5.43	5.57	5.51	5.77
K_2O	2.38	2.85	3.29	2.84	3.05	2.58	2.71	2.37	2.74	2.50	2.63	2.73	2.40	2.48
NiO	0.00	0.02	0.00	0.01	0.00	0.00	0.01	0.01	0.01	0.01	0.01	0.00	0.01	0.01
P_2O_5	0.35	0.40	0.00	0.41	0.18	0.39	0.40	0.34	0.41	0.36	0.36	0.40	0.29	0.40
Hydrous total	98.12	98.10	97.16	100.25	95.20	97.06	96.11	97.25	93.13	90.99	95.71	93.36	98.12	91.04

	Amphibole						Garnet			Clinopyroxene				
Experiment	1	4	5	6	12	14	2	9	13	1	2	4	5	6
***n*=**	*7*	*14*	*6*	*15*	*8*	*18*	*6*	*7*	*18*	*6*	*6*	*6*	*8*	*5*
SiO_2	44.31	43.77	44.30	44.17	44.45	45.59	40.53	40.45	40.13	52.91	51.75	51.08	52.80	52.68
TiO_2	2.36	2.18	1.92	1.79	2.14	1.84	1.16	0.70	1.45	0.63	0.68	0.78	0.56	0.57
Al_2O_3	13.64	12.58	14.20	12.49	11.48	11.91	22.22	22.52	21.23	6.03	8.22	4.58	4.64	2.71
Cr_2O_3	0.13	0.12	0.13	0.10	0.14	0.28	0.09	16.59	0.08	0.20	-	0.22	0.21	0.11
FeO	8.47	10.92	9.16	10.05	8.90	6.26	16.55	0.47	17.56	6.44	7.15	8.02	7.38	8.29
MnO	0.13	0.13	0.12	0.13	0.12	0.10	0.48	13.34	0.53	0.18	0.16	0.24	0.18	0.35
MgO	15.45	14.37	15.11	15.03	16.11	17.65	13.52	7.19	12.26	15.02	13.47	15.63	15.86	14.58
CaO	10.00	10.58	10.43	10.92	11.32	10.63	6.68	0.03	6.55	17.71	16.58	18.24	18.85	20.39
Na_2O	3.13	2.63	3.00	2.74	2.62	3.01	0.11	0.01	0.24	1.25	2.17	0.95	1.00	0.66
K_2O	0.92	0.78	1.01	0.89	0.78	1.02	0.01	0.19	0.01	0.12	0.04	0.17	0.01	0.08
NiO	0.09	0.01	0.06	0.04	0.04	0.02	0.02	0.02	0.02	0.03	0.00	0.02	0.04	0.00
P_2O_5	0.00	0.08	0.07	0.03	0.03	0.02	0.18	0.08	0.27	0.00	0.00	0.03	0.02	0.06
H_2O	*2.00*	*2.00*	*2.00*	*2.00*	*2.00*	*2.00*	-	-	-	-	-	-	-	-
Total	100.64	100.16	101.52	100.40	100.13	100.32	101.53	101.58	100.33	100.52	100.22	99.98	101.55	100.47

	Clinopyroxene (continued)						Orthopyroxene						Ol
Experiment	9	10	11	12	13	14	1	2	5	10	11	14	12
***n*=**	*11*	*13*	*8*	*6*	*4*	*15*	*6*	*4*	*3*	*11*	*4*	*4*	*5*
SiO_2	52.19	52.88	53.14	53.75	55.54	53.29	53.84	52.19	54.31	54.42	56.39	55.76	39.44
TiO_2	0.58	0.43	0.43	0.43	1.21	0.43	0.28	0.25	0.20	0.17	0.33	0.16	0.03
Al_2O_3	5.69	3.93	5.05	2.25	11.11	3.30	4.57	7.14	4.28	3.49	6.17	1.81	0.20
Cr_2O_3	0.17	0.23	0.25	0.20	0.07	0.23	0.10	0.15	0.19	0.21	0.06	0.21	0.02
FeO	8.12	7.37	5.60	6.23	7.72	5.81	13.88	13.88	13.31	13.82	6.94	11.19	20.60
MnO	0.19	0.23	0.16	0.20	0.15	0.18	0.26	0.24	0.20	0.21	0.20	0.23	0.24
MgO	15.45	15.92	16.56	16.50	10.33	16.92	26.14	25.47	27.13	26.73	25.27	29.36	39.39
CaO	17.28	18.93	17.84	20.43	9.09	19.26	1.63	1.18	1.50	1.78	3.15	1.33	0.22
Na_2O	1.14	0.87	1.05	0.41	2.72	0.84	0.17	0.23	0.13	0.14	0.73	0.08	0.04
K_2O	0.02	0.04	0.04	0.03	1.46	0.01	0.04	0.02	0.02	0.04	0.48	0.01	0.03
NiO	0.02	0.05	0.03	0.01	0.05	0.02	0.05		0.03	0.09	0.02	0.02	0.07
P_2O_5	0.02	0.03	0.03	0.03	0.20	0.02	0.00	0.07	0.00	0.02	0.09	0.01	0.13
H_2O	-	-	-	-	-	-	-	-	-	-	-	-	-
Total	100.86	100.92	100.20	100.49	99.65	100.30	100.96	100.84	101.31	101.11	99.83	100.18	100.42

table

Click here to download table: Table 4 Cumulate modelling.xls

Table 4 Fractionation and bulk cumulate residue calculation. The most primitive composition from Table 1 is used as a parent magma, and the most felsic sample as the daughter magma. Fractionating phase compositions taken from experimentally produced minerals, plus an andesine core (An_{43}) composition from sample 357461. This is used as no plagioclase data are available from experiments, and the cumulate requires a more silica-rich phase in order to model felsic adakitic compositions at acceptable R^2 levels. M = [MgO+FeO]*[40.32/71.85] + MnO*[40.32/70.94]. A fractionating assemblage of 21% amphibole, 6% clinopyroxene and 23% plagioclase can produce the compostions of the Surigao magmas (Figure 5).

	Amph	Cpx	Andesine	Daughter	Parent	Sum of reactants	R^2	Bulk cumulate
	Exp 1	Exp 2	357461	357417	357433			
SiO_2	46.81	53.35	58.20	64.62	58.73	58.73	0.00	52.84
TiO_2	2.50	0.70	0.00	0.51	0.83	0.82	0.00	1.13
Al_2O_3	14.42	8.48	26.43	18.27	18.44	18.75	0.10	19.23
M	21.42	18.12	0.07	4.65	7.71	7.93	0.05	11.20
CaO	10.56	17.09	8.71	4.08	7.56	7.29	0.07	10.49
Na_2O	3.31	2.23	6.27	5.00	4.76	4.77	0.00	4.54
K_2O	0.97	0.04	0.31	2.86	1.97	1.71	0.07	0.55
Total	100	100	100	100	100	100	0.29	100
Melt fraction	0.21	0.06	0.23	0.50				